Experimental report

30/03/2017

Proposal: **INTER-364** **Council:** 10/2016

Title: Internal time on SALSA

Research area:

This proposal is a new proposal

Main proposer: **Thilo PIRLING**

Experimental team: Cui Er SEOW
Harry COULES

Local contacts: Thilo PIRLING

Samples: FeNiAl

Instrument	Requested days	Allocated days	From	To
SALSA	5	5	06/02/2017	11/02/2017

Abstract:

Experimental investigation of the effects of material anisotropy on applied strain evolution in Wire and Arc Additively Manufactured nickel-base alloys

Experiment: INTER-364
Experimental team: Harry Coules, Cui Er Seow
Department of Mechanical Engineering, University of Bristol & National Structural Integrity Research Centre

Introduction

Wire and Arc Additive Manufacturing (WAAM) is a technique that enables large metallic structures to be built up quickly with much less material wastage due to its high deposition rates [1]. The process, which utilises a wire feedstock and welding arc as a heat source, causes the part to undergo complex thermal cycling, promoting epitaxial crystallite growth and hence anisotropic material properties [2]. Relatively little is known about the micro (grain size, texture, phase transformation) and macroscale properties (yield and tensile strength, fracture toughness) of the deposited metal, for most material systems. The goal of our work is to find ways to deal with WAAM parts within fracture-mechanics-based structural integrity assessment methods. An important step in this is to understand the influence of microstructure on the mechanical behaviour of WAAM materials. In this experiment, we characterised the applied strain field in two fracture specimens, each with a crack in different directions with respect to the build direction. In order to prevent the pseudostrain effect in this coarse grained material, we developed a method to track individual crystallites as the material deformed. The results will be compared against a detailed microstructure analysis on the deformed specimens to understand the interactions between grains when the material yields.

Method

Two Compact Tension (C(T)) specimens were extracted from wire and arc additively manufactured Inconel 625. They were notched using wire Electrical Discharge Machining (EDM) and fatigue pre-cracked as per ASTM E1820 in two different directions, one parallel to the build direction and the other perpendicular. The specimens were set up in a 50kN loading rig, which enabled the specimen to be loaded in displacement control. The load and Crack Mouth Opening Displacement (CMOD) of the specimens were measured using a clip gauge. In parallel, Digital Image Correlation (DIC) was used to observe the total strain of the specimens. The specimen geometry, measurement grid and experimental set up are shown in Figure 1(a) and (b) respectively.

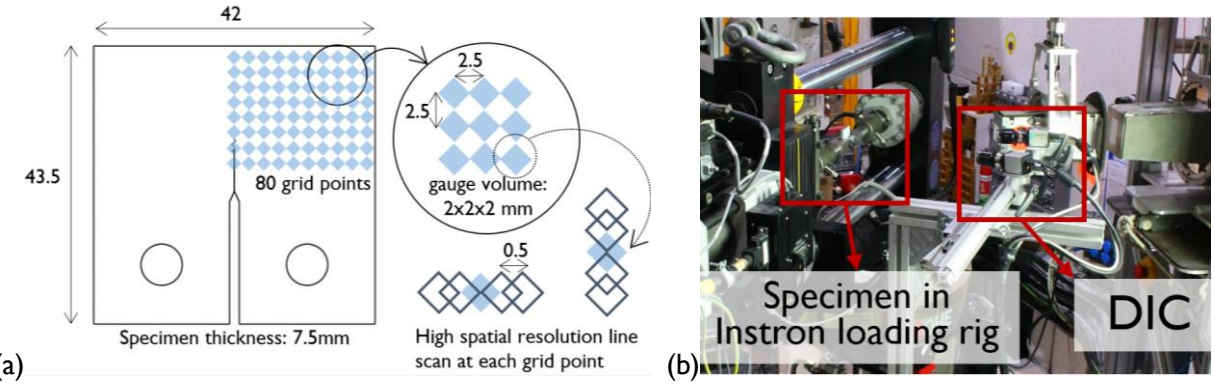

Figure 1: (a) Geometry of the C(T) specimens and the measurement grid used (b) Setup with 50kN loading rig and DIC cameras on SALSA

Measurements of applied elastic strain in the crack transverse direction were made using SALSA. The specimens were loaded up in several loading increments. The measurement before the first loading increment was taken to be the reference (i.e. initial d-spacing). Subsequently, measurements were made after each loading increment. All measurements were made with an incoming neutron wavelength of 1.61 Å and a gauge volume of 2x2x2 mm. The material was found to be strongly textured, where only the {200} reflection gave good Bragg peaks and hence was the reflection observed for all measurements.

As the grains in the material were observed to be very large, instead of treating the material as a powder, the specimen was positioned such that each measurement point was wholly within a single crystallite. This was done by firstly setting up a grid as shown in Figure 1(a), then making a high resolution line scan to the sides and above each grid point. Points with noticeable peak shifts indicated that they are only partially filled by one crystallite. These grid points identified were eliminated from the original grid to avoid pseudo strain effects in the results. It was observed that in CT1, there were 21 points of the original grid which were suitable for measurements. In CT3, all 80 points were observed to be within single crystallites.

After each loading increment, due to the deformation of the material, the positions of these crystallites changed with respect to the position of the beam. Using DIC data, the displacements of each point were obtained and incorporated into the coordinates of the hexapod on SALSA. This ensured that the same points on the specimen were measured at different loading increments.

Two types of neutron diffraction measurements were taken, one is the standard grid scan where the loading of the specimen was paused at set increments (as described above) to obtain a strain field. The second type is a list mode scan, which measures a single point throughout during each loading increment. For both specimens, the point with XY specimen coordinates (2, -4) was chosen.

Results

The applied elastic strain field in CT1 and CT3 are shown in Figures 2 and 3 respectively. The results show that the measurements have not been affected by pseudo strain effects, which means that the method of crystallite tracking has been successful. As expected, a region of tension can be observed ahead of the crack tip, and a region of compression can be observed on the back face of the CT specimen. From the plot at CMOD = 0mm in Figure 2, it can be observed that near the centre of the plot (i.e. points reading approx. 1000 μstrain) are in tension at a fairly low load. Observing the same points with increasing CMOD shows that the strain at these points first increase then decrease, some of which even reach compressive values at CMOD=3.6mm. This trend is shown in more detail on graphs of microstrain vs. CMOD for each measurement point in Figure 4(a), where it can be seen that the decrease in strain begins from about CMOD = 1mm. One explanation for this trend is that those points are all within a single crystallite, and the deformation of this crystallite has been inhibited by the deformation of the surrounding crystallites.

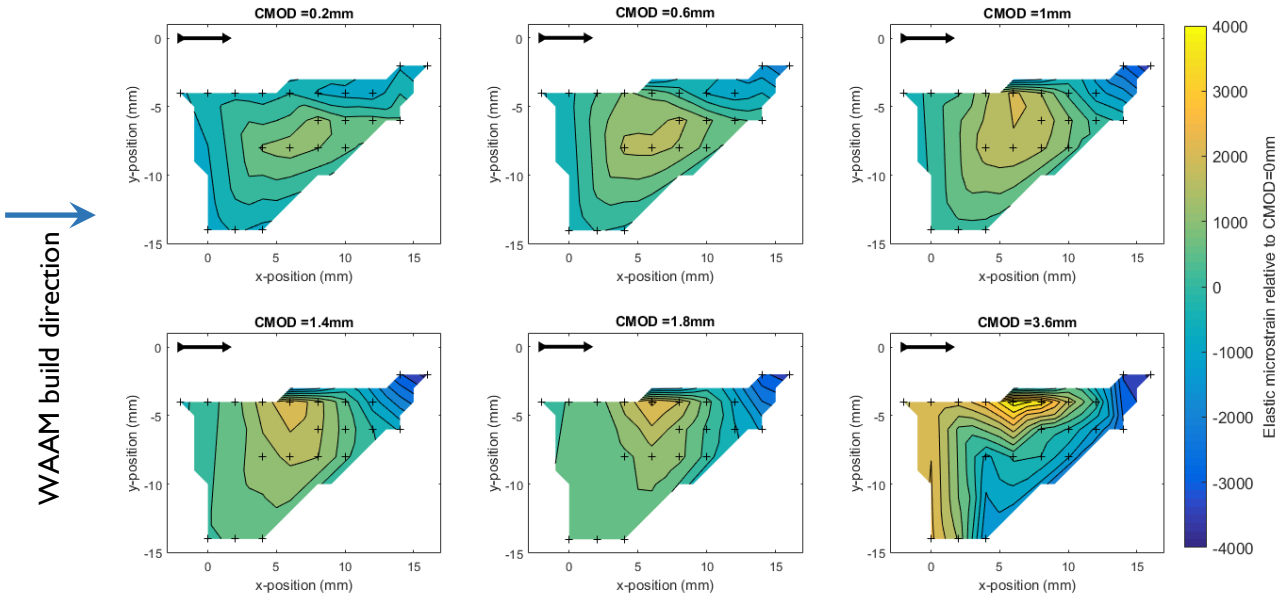

Figure 2: Contour plots of the applied elastic microstrain field in one half of CT1 at each CMOD increment. The black double ended arrow, which represents the EDM notch and fatigue pre-crack, points in the direction of crack propagation. The build direction of the WAAM sample is also indicated by the blue single ended arrow. Measurement points are represented by the crosses.

In contrast, this trend is not seen in the plots for CT3. All points show monotonically increasing or decreasing strain values, which is also seen in the graphs of microstrain vs. CMOD in Figure 4(b). These results will be matched up with a detailed microstructural analysis on the deformed specimens, where the strain field will be mapped to individual grains within the material. A relationship between microstructure and elastic strain will be developed. These results will also be compared against DIC data, which gives the total strain of the specimen and can be used to decouple elastic and plastic deformation at a microscale level. A procedure for analysing data from list mode scans have not yet been developed and hence data from these scans have not been analysed. However, we are working with the beamline scientist to develop this.

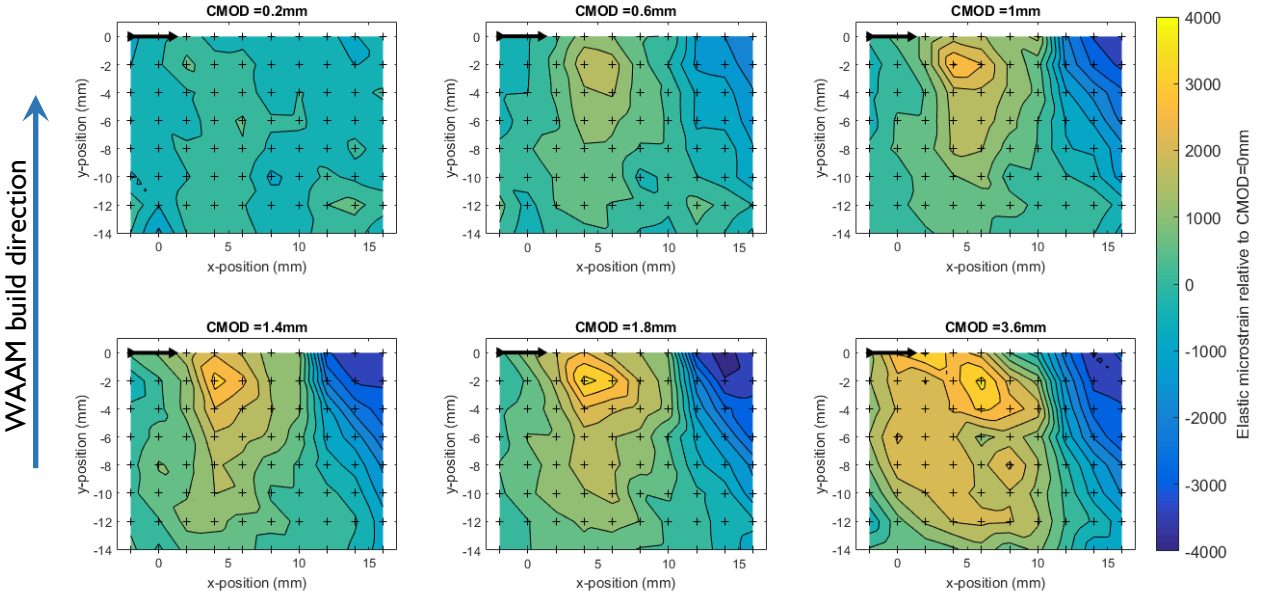

Figure 3: Contour plots of the applied elastic microstrain field in one half of CT3 at each CMOD increment. The black double ended arrow, which represents the EDM notch and fatigue pre-crack, points in the direction of crack propagation. The build direction of the WAAM sample is also indicated by the blue single ended arrow. Measurement points are represented by the crosses.

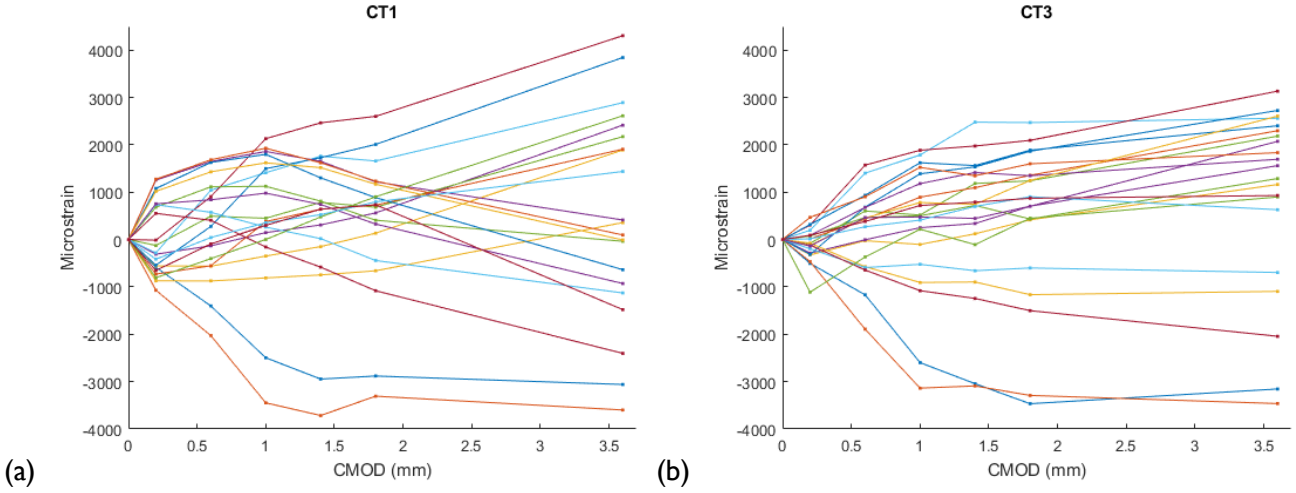

Figure 4: Evolution of applied strain with increasing CMOD, showing data from selected points for (a) CT1, showing some points with strain increasing then decreasing at CMOD=1mm and (b) CT, showing monotonically increasing elastic strain for all points.

[1] S. W. Williams, F. Martina, A. C. Addison, J. Ding, G. Pardal, and P. Colegrove, "Wire+ arc additive manufacturing," *Materials Science and Technology*, vol. 32, no. 7, pp. 641–647, 2016.

[2] F. D. Wang, S. Williams, P. Colegrove, and A. A. Antonysamy, "Microstructure and Mechanical Properties of Wire and Arc Additive Manufactured Ti-6Al-4V," *Metallurgical and Materials Transactions a-Physical Metallurgy and Materials Science*, vol. 44a, no. 2, pp. 968–977, 2013.